# TGF-β inhibitor Smad7 regulates dendritic cell-induced autoimmunity

Dominika Lukas[a], Nir Yogev[a], Junda M. Kel[b], Tommy Regen[a], Ilgiz A. Mufazalov[a], Yilang Tang[a], Florian Wanke[a], Boris Reizis[c], Werner Müller[d], Florian C. Kurschus[a], Marco Prinz[e,f], Ingo Kleiter[g], Björn E. Clausen[a,b,1,2], and Ari Waisman[a,1,2]

[a]Institute for Molecular Medicine, University Medical Center of the Johannes Gutenberg University Mainz, 55131 Mainz, Germany; [b]Department of Immunology, Erasmus MC, University Medical Center Rotterdam, 3015 GE Rotterdam, The Netherlands; [c]Department of Pathology, New York University School of Medicine, New York, NY 10016; [d]Faculty of Biology, Medicine and Health, University of Manchester, Manchester M13 9PT, United Kingdom; [e]Institute of Neuropathology, Faculty of Medicine, University of Freiburg, 79106 Freiburg, Germany; [f]BIOSS Centre for Biological Signalling Studies, University of Freiburg, 79104 Freiburg, Germany; and [g]Department of Neurology, St. Josef-Hospital, Ruhr-University Bochum, 44791 Bochum, Germany

Edited by Scott S. Zamvil, University of California, San Francisco, CA, and approved by Editorial Board Member Tak W. Mak December 31, 2016 (received for review September 12, 2016)

**TGF-β is an anti-inflammatory cytokine whose signaling is negatively controlled by Smad7. Previously, we established a role for Smad7 in the generation of autoreactive T cells; however, the function of Smad7 in dendritic cells (DCs) remains elusive. Here, we demonstrate that DC-specific Smad7 deficiency resulted in elevated expression of the transcription factors Batf3 and IRF8, leading to increased frequencies of $CD8^+CD103^+$ DCs in the spleen. Furthermore, Smad7-deficient DCs expressed higher levels of indoleamine 2,3-dioxygenase (IDO), an enzyme associated with tolerance induction. Mice devoid of Smad7 specifically in DCs are resistant to the development of experimental autoimmune encephalomyelitis (EAE) as a result of an increase of protective regulatory T cells (Tregs) and reduction of encephalitogenic effector T cells in the central nervous system. In agreement, inhibition of IDO activity or depletion of Tregs restored disease susceptibility. Intriguingly, when Smad7-deficient DCs also lacked the IFN-γ receptor, the mice regained susceptibility to EAE, demonstrating that IFN-γ signaling in DCs mediates their tolerogenic function. Our data indicate that Smad7 expression governs splenic DC subset differentiation and is critical for the promotion of their efficient function in immunity.**

conditional gene targeting | dendritic cells | EAE | Smad7 | tolerance induction

Transforming growth factor (TGF)-β is a pleiotropic cytokine essential for immune homeostasis and tolerance. Systemic loss of TGF-β results in lethal multiorgan autoimmunity as a result of destructive autoreactive leukocyte infiltration into various organs (1–5). TGF-β signaling is tightly regulated to ensure equilibrium of the immune system. Smad7 is a potent negative regulator of TGF-β signaling and prevents the binding of Smad2 and Smad3 to the TGF-β receptor II, which is required for TGF-β signal transduction. In addition, together with Smurf, Smad7 targets the TGF-β receptor for proteasomal degradation, which results in the termination of TGF-β signaling (6). Although Smad7 is expressed upon TGF-β signaling, other stimuli such as interferon (IFN)-γ can induce Smad7 expression (7).

Dendritic cells (DCs) are professional antigen-presenting cells that constantly sample their environment for foreign and self-antigens and thus play a prominent role in balancing immunity vs. tolerance (8, 9). DCs constitute a heterogeneous family of cells consisting of two main populations, namely conventional DCs and plasmacytoid DCs (pDCs). Conventional DCs are mainly composed of $CD11b^+$, $CD8^+$, and $CD103^+$ subsets. DC development and subset differentiation are governed by the orchestrated expression of specific transcription and growth factors (10, 11). Development of $CD8^+$ and $CD103^+$ DCs is dependent on expression of the transcription factors Batf3 (basic leucine zipper transcriptional factor ATF-like 3) and IRF8 (interferon regulatory factor 8), yet stimuli that induce or repress their expression in vivo remain poorly defined (12, 13). $CD8^+$ and $CD103^+$ DCs contribute to central (14), as well as peripheral tolerance induction in part because of their ability to produce high amounts of TGF-β (11, 15, 16). In general, DCs can secrete and respond to TGF-β and stimulation with TGF-β in vitro retained DCs in an immature state (17). In contrast, conditional deletion of the TGF-β receptor II in DCs did not alter DCs maturation in vivo but resulted in the spontaneous development of autoimmunity (18), highlighting the importance for TGF-β signaling specifically in DCs for the maintenance of tolerance. TGF-β can induce indoleamine 2,3-dioxygenase (IDO) expression in DCs (19); IDO is an enzyme involved in tryptophan catabolism with immunosuppressive functions (20). During inflammation, IDO expression can also be induced by IFN-γ (19), thereby limiting excessive immune reactions. To date, it has not been addressed to our knowledge whether Smad7 signaling in DCs is involved in the regulation of IDO expression.

Experimental autoimmune encephalomyelitis (EAE) represents a murine model for multiple sclerosis (MS) in which CNS-autoreactive T cells induce a demyelinating disease. Although DCs play an important role in inducing CNS-autoreactive T cells (21), ablation or absence of CD11c-positive DCs results in exacerbated disease progression, suggesting an additional

## Significance

**Smad7 is a negative regulator of TGF-β signaling, a cytokine with anti-inflammatory properties. Although TGF-β was implicated in the development and function of dendritic cells (DCs), the in vivo role of Smad7 in DCs remains elusive. Here, we demonstrate that DC-specific Smad7 deletion affects the development of splenic $CD8^+CD103^+$ DCs by regulating expression of the transcription factors Batf3 and IRF8. In addition, Smad7 directs DC function by regulating the expression of indoleamine 2,3-dioxygenase in response to IFN-γ signaling. Hence, absent Smad7 in DCs mediates resistance of mice to the development of autoimmunity via protective regulatory T-cell induction. These findings demonstrate that Smad7 expression governs splenic DC subset differentiation and affects tolerogenic DC function in vivo.**

Author contributions: D.L., N.Y., F.C.K., M.P., I.K., B.E.C., and A.W. designed research; D.L., N.Y., J.M.K., T.R., I.A.M., Y.T., and F.W. performed research; B.R., W.M., and I.K. contributed new reagents/analytic tools; D.L., N.Y., J.M.K., T.R., I.A.M., F.C.K., M.P., and B.E.C. analyzed data; and D.L., N.Y., B.E.C., and A.W. wrote the paper.

The authors declare no conflict of interest.

This article is a PNAS Direct Submission. S.S.Z. is a Guest Editor invited by the Editorial Board.

[1]B.E.C. and A.W. contributed equally to this work.

[2]To whom correspondence may be addressed. Email: waisman@uni-mainz.de or bclausen@uni-mainz.de.

This article contains supporting information online at www.pnas.org/lookup/suppl/doi:10.1073/pnas.1615065114/-/DCSupplemental.

regulatory function of DCs during EAE (22). Mice harboring DCs with impaired TGF-β receptor II signaling exhibit increased susceptibility to EAE and develop a more severe course of disease (23). Moreover, elevated Smad7 levels were detected in T cells from patients with MS at the stage of active disease, as well as in mice subjected to EAE (24). Thus far, the role of Smad7 in DCs during steady state and EAE remains elusive.

By using DC-specific Smad7-KO mice, we reveal a function of Smad7 as regulator of Batf3- and IRF8-mediated development of $CD8^+CD103^+$ splenic DCs. Moreover, we demonstrate a critical role of Smad7 in inhibition of IDO-driven Treg induction able to

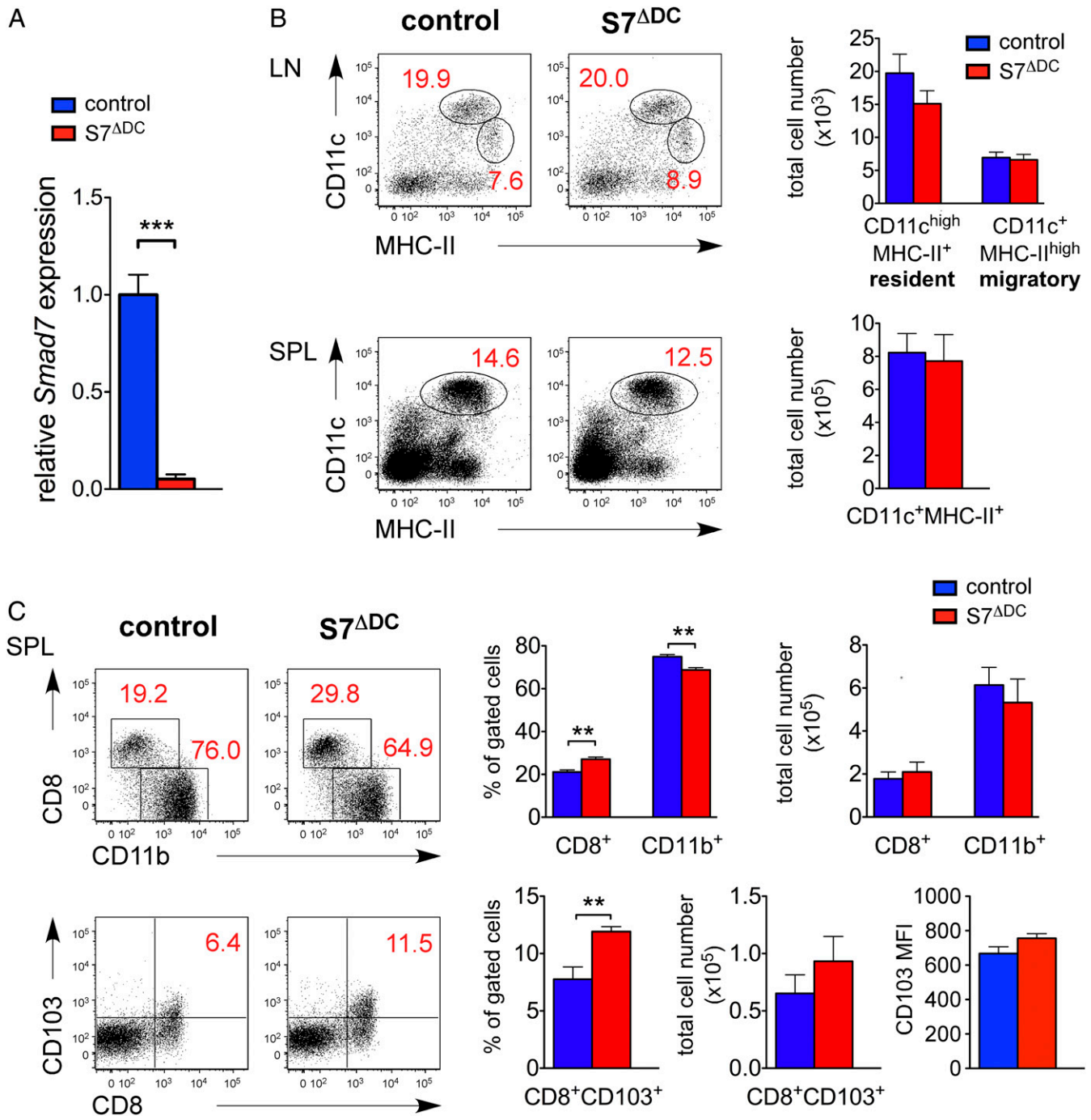


**Fig. 1.** Smad7 deletion in DCs leads to increased frequencies of splenic $CD8^+CD103^+$ DCs. (*A*) Real-time PCR analysis of Smad7 expression levels relative to HPRT of purified splenic $CD11c^+$ DCs isolated from $S7^{\Delta DC}$ ($n = 4$) or control animals ($n = 4$). One representative of five independent experiments is depicted. (*B*) FACS plots and total cell counts of inguinal LN (*Upper*) and splenic DCs (*Lower*) derived from $S7^{\Delta DC}$ ($n = 7$) or controls ($n = 6$). Cells were gated on $CD90.2^-B220^-$ cells. One representative of five independent experiments is shown. (*C*) FACS blots and frequencies of splenic DC subsets as gated on $CD90.2^-B220^-CD11c^+MHCII^+$ cells of $S7^{\Delta DC}$ ($n = 7$) or control mice ($n = 6$). CD103 MFI of splenic DCs as gated on $CD11c^+MHCII^+CD8^+CD103^+$ cells of $S7^{\Delta DC}$ ($n = 7$) or control mice ($n = 6$) is depicted. One representative of three independent experiments is depicted. Bar graphs depict mean value ± SEM. Statistical significance was assessed by using Student's *t* test (*$P \leq 0.05$, **$P \leq 0.005$, and ***$P \leq 0.0005$).

attenuate disease outcome of EAE, and we show that IFN-γ signaling in DCs is necessary for tolerance induction by Smad7-deficient DCs.

## Results

**Smad7 Deficiency Enhances the Development of CD8$^+$CD103$^+$ DCs in the Spleen.** To study the role of Smad7 in DCs, we generated mice with a DC-specific deletion of Smad7 (S7$^{\Delta DC}$) by crossing a conditional Smad7 allele (24) to CD11c-Cre (25) mice. Splenic CD11c$^+$ DCs from homozygous S7$^{\Delta DC}$ mice exhibited an almost complete loss of Smad7 mRNA as determined by quantitative real-time (RT)-PCR (Fig. 1*A*), demonstrating efficient target gene deletion. Next, we investigated whether Smad7 deficiency affects DCs during the steady state but did not observe any significant differences in the frequency and total number of splenic CD11c$^+$ MHC-II$^+$ DCs. Similarly, resident CD11c$^{high}$MHC-II$^+$ and migratory CD11c$^+$MHC-II$^{high}$ DCs in lymph nodes (LNs) of S7$^{\Delta DC}$ mice were comparable to controls (Fig. 1*B*). When we further analyzed splenic DC subsets in more detail, we detected a significant increase in the proportion of CD8$^+$ DCs and, in particular, the CD8$^+$CD103$^+$ DC subset involved in tolerance induction (11, 14–16) (Fig. 1*C*, *Lower*). In contrast, we did not notice any changes in the composition of DC subsets in the LN (Fig. S1*A*). Moreover, frequencies and total cell counts of pDCs in LN and spleen of naïve mutant mice were indistinguishable from those in WT controls (Fig. S1*B*). Notably, although TGF-β induces CD103 surface expression on CD8$^+$ T cells (26–28), CD103 expression levels by Smad7-deficient splenic CD8$^+$CD103$^+$ DCs were not affected (Fig. 1*C*, *Lower Right*), indicating genuine expansion of this DC subset. Furthermore, Smad7 deficiency did not alter the expression of MHC class II (MHC-II) or CD80/86 by DCs (Fig. S1*C*). Taken together, these data indicate that lack of Smad7 does not affect DC homeostasis and maturation in the steady state, except for the increased frequency of CD8$^+$CD103$^+$ tolerogenic splenic DCs, which might be important in the context of immune challenge.

**Increased Expression of the Transcription Factors Batf3 and IRF8 by Smad7-Deficient CD8$^+$ and CD103$^+$ Splenic DCs.** As S7$^{\Delta DC}$ mice harbored increased frequencies of CD8$^+$CD103$^+$ splenic DCs during the steady state, we investigated whether loss of Smad7 affects the expression of IRF8 or Batf3, two transcription factors mandatory for CD8$^+$CD103$^+$ DC development (12, 13). Previously, it was demonstrated that TGF-β induces IRF8 expression in DCs, which is inhibited by Smad7 overexpression (29). Similarly, IFN-γ stimulation induces IRF8 expression during inflammation (30, 31). However, it is not yet clear which stimuli control expression of Batf3. Therefore, we isolated splenic DCs from S7$^{\Delta DC}$ mice and treated them for 24 h with TGF-β or IFN-γ. Quantitative RT-PCR analysis revealed significantly increased expression of *Irf8* in splenic S7$^{\Delta DC}$ DCs under both stimulation conditions compared with control cells (Fig. 2 *A* and *C*), indicating that Smad7 affects transcriptional factors controlling DC lineage commitment in the spleen. As depicted in Fig. 2 *B* and *D*, TGF-β and IFN-γ induced expression of *Batf3* in splenic DCs, which was elevated in cells lacking Smad7. Taken together, these data indicate that Smad7 is a negative regulator of *Batf3* and *Irf8* expression, and its absence promotes the development of Batf3- and IRF8-dependent splenic CD8$^+$CD103$^+$ DCs in S7$^{\Delta DC}$ mice.

**Lack of Smad7 in DCs Does Not Affect T-Cell Homeostasis in the Steady State.** Next, we tested whether loss of Smad7 in DCs affected T-cell development, subset differentiation, or activation during the steady state. Deletion of Smad7 in DCs had no impact on T-cell development in the thymus (Fig. S2*A*, *Upper*). Likewise, the splenic B/T-cell ratio was comparable between S7$^{\Delta DC}$ and control animals

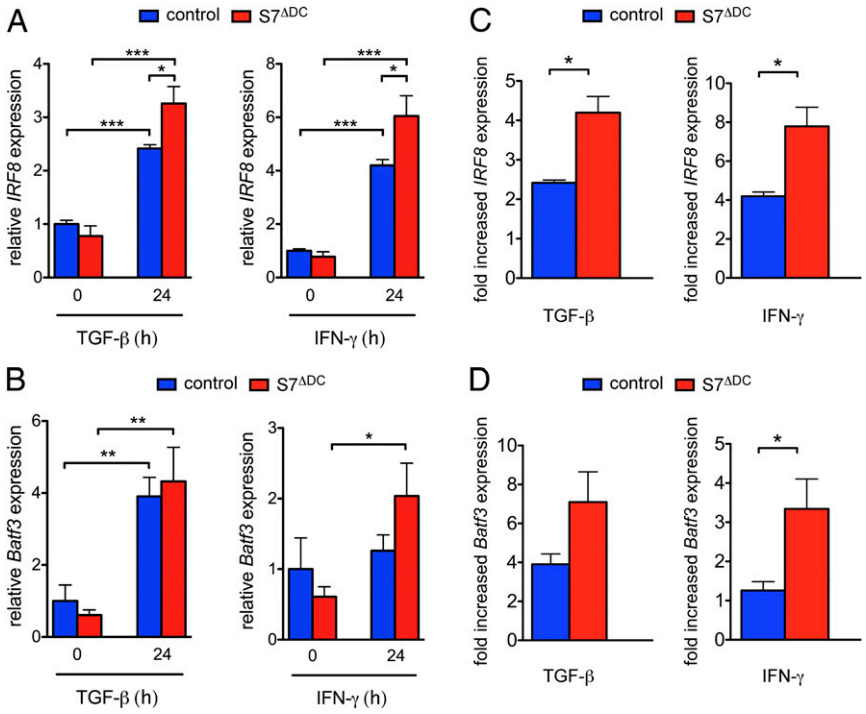


**Fig. 2.** Smad7 controls the expression of the transcription factors Batf3 and IRF8, which drive CD8$^+$CD103$^+$ DC development. Real-time analysis of IRF8 (*A*) and Batf3 (*B*) expression in purified splenic CD11c$^+$ DCs derived from untreated S7$^{\Delta DC}$ ($n = 4$) or control animals ($n = 4$), stimulated with 10 ng/mL IFN-γ or 10 ng/mL TGF-β for 24 h or left untreated. (*C* and *D*) Fold increase in IRF8 (*C*) and Batf3 (*D*) expression in response to the stimuli depicted in *A* and *B*. (*A*–*D*) One representative of two independent experiments is depicted. Bar graphs depict mean value ± SEM. Statistical significance was assessed by using two-way ANOVA and Bonferroni posttests (*$P \leq 0.05$, **$P \leq 0.005$, and ***$P \leq 0.0005$).

(Fig. S2*A*, *Middle*). In accordance with the unaltered expression of MHC-II and costimulatory molecules by Smad7-deficient DCs, no difference in the activation status of $CD4^+$ T cells could be detected. The total number of naïve, effector, and memory $CD4^+$ T cells was unaltered in $S7^{\Delta DC}$ mice compared with controls (Fig. S2*A*, *Lower*). Notably, despite the increased frequency of $CD8^+CD103^+$ splenic DCs, cells that were previously implicated in tolerance induction (11, 14–16), the numbers of Tregs in LN and spleens of $S7^{\Delta DC}$ mice remained similar to controls (Fig. S2*B*). In conclusion, loss of Smad7 specifically in DCs does not affect T-cell homeostasis during the steady state.

**DCs Devoid of Smad7 Mediate Resistance to EAE.** As $S7^{\Delta DC}$ mice exhibited increased levels of $CD8^+CD103^+$ splenic DCs previously associated with tolerance induction, we asked whether the lack of Smad7 in DCs could influence autoimmunity. We therefore induced active EAE in these mice by using myelin oligodendrocyte glycoprotein $(MOG)_{35–55}$ peptide. Intriguingly, $S7^{\Delta DC}$ mice were resistant to EAE compared with control animals (Fig. 3*A*). When we analyzed the CNS of these mice at the peak of disease, we detected a significant decrease in CNS-infiltrating $CD90.2^+$ T cells (Fig. 3*B*) and, among them, a significant reduction in $CD4^+$ T cells compared with control mice (Fig. 3*C*, *Upper*). To determine the level of $MOG_{35–55}$–specific effector $CD4^+$ T cells infiltrating the CNS of $S7^{\Delta DC}$ mice, we restimulated CNS-infiltrating cells with $MOG_{35–55}$ peptide and measured the expression of CD40 ligand (CD40L), which is transiently expressed upon T-cell activation (32). We found that the lower number of T cells in the CNS of the $S7^{\Delta DC}$ mice was the result of a reduction in antigen-specific $CD4^+$ T cells (Fig. 3*C*, *Middle*). Although there was no difference in the ratios of antigen-specific Th1 and Th17 cells or IL-17A and IFN-γ double producers, total cell counts exhibited fewer CNS-infiltrating Th1 and Th17 cells and significantly fewer T cells producing IL-17A and IFN-γ in $S7^{\Delta DC}$ mice (Fig. 3*C*, *Bottom*). Together, these data indicate that deletion of Smad7 in DCs attenuates the differentiation and infiltration of pathogenic T-cell populations into the CNS. As we have previously shown, DCs directly affect the development of peripherally induced Tregs during EAE (22). In agreement, we detected increased numbers of Tregs in $S7^{\Delta DC}$ mice in secondary lymphoid organs and significantly increased percentages of Tregs in the CNS (Fig. 3*D*). In conclusion, loss of Smad7 in DCs reduces the susceptibility of mice to EAE, probably as a result of an enlarged Treg compartment.

**T-Cell Priming During EAE Is Independent of Smad7 Expression in DCs.** Next we sought to assess whether disease resistance of $S7^{\Delta DC}$ mice might also result from impaired T-cell priming. As antigen uptake and presentation by DCs is a crucial step in eliciting an immune response, we addressed whether loss of Smad7 might affect the antigen presentation capacity of DCs. Therefore, we induced EAE in $S7^{\Delta DC}$ and control mice by s.c. immunization with $MOG_{35–55}$/Complete Freund's Adjuvant (CFA) emulsion containing beads labeled with FITC, which enabled us to identify $FITC^+$ DCs after antigen uptake and follow their migration to the draining LN (dLN). Analysis of these mice 1, 2, and 3 d after immunization revealed a similar frequency of FITC-labeled $CD11c^+MHC\text{-}II^+$ DCs in the dLN of $S7^{\Delta DC}$ and control mice (Fig. S3*A*), indicating that DC antigen uptake and migration was not affected by the deletion of Smad7. Further in vitro analysis revealed unaltered secretion of TGF-β by Smad7-deficient DCs upon stimulation with LPS and CD40L (Fig. S3*B*). Next, we investigated whether DC maturation might be altered in the absence of Smad7. Mice were immunized with the $MOG_{35–55}$ peptide, and the activation status of $CD11c^+MHC\text{-}II^{high}$ migratory DCs present in the dLN was monitored on a daily basis. We did not detect any difference in CD80 or CD86 expression between Smad7-deficient and control DCs, as indicated by their similar mean fluorescence intensity

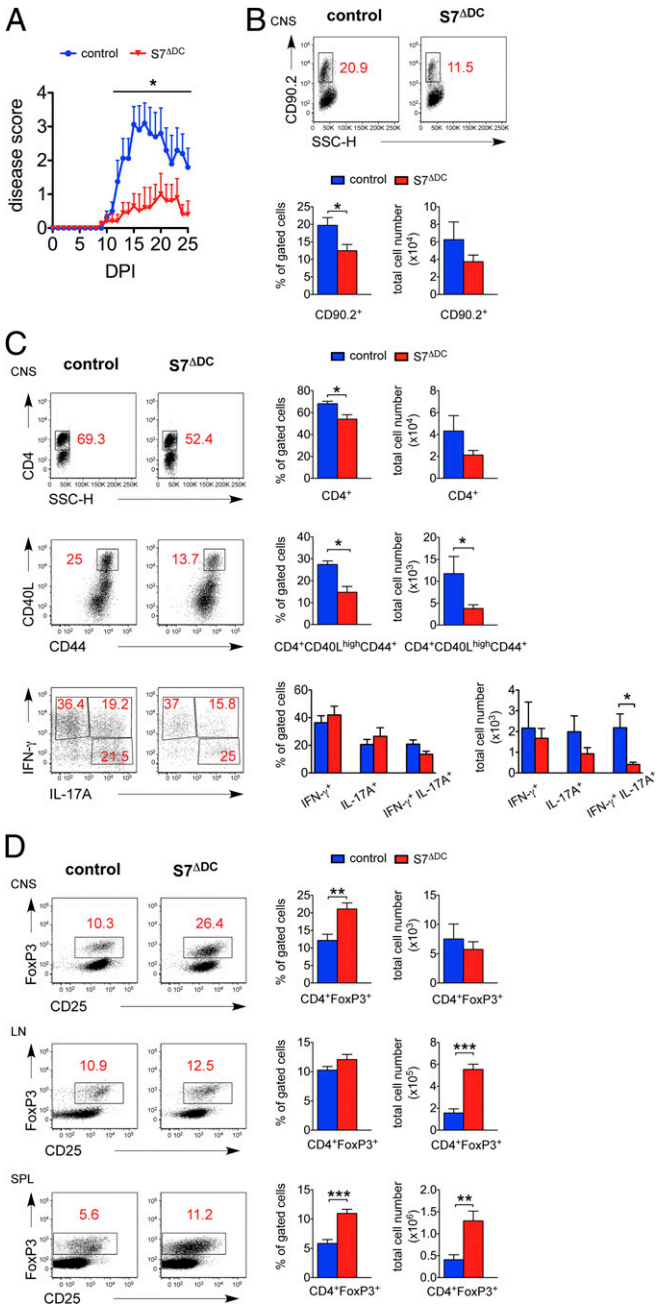


**Fig. 3.** DC-specific Smad7 deletion renders mice resistant to EAE. (*A*) EAE disease course of $S7^{\Delta DC}$ ($n = 10$) and control animals ($n = 8$) after $MOG_{35–55}$/CFA and PTX immunization. One representative of five independent experiments is shown. (*B*) Flow cytometric analysis of CNS-infiltrating $CD90.2^+$ T cells from $S7^{\Delta DC}$ ($n = 8$) and control mice ($n = 7$) at the peak of disease (day 15). Cells were gated on live cells. One representative of four independent experiments is depicted. (*C*) FACS blots of CNS-infiltrating $CD4^+$ T cells from $S7^{\Delta DC}$ ($n = 8$) and control mice ($n = 7$) at the peak of disease (day 15; *Upper*). $MOG_{35–55}$–specific CNS-infiltrating effector T cells ($CD40L^{high}CD44^+$) pregated on $CD90.2^+CD4^+$ cells (*Middle*). $MOG_{35–55}$–specific CNS-infiltrating Th1 ($IFN\text{-}\gamma^+$) and Th17 ($IL\text{-}17A^+$) effector cells were pregated on $CD90.2^+CD4^+CD40L^{high}CD44^+$ cells (*Lower*). (*D*) Percentage and total cell counts of CNS-infiltrating $FoxP3^+$ Tregs (*Upper*) and LN and splenic $Foxp3^+$ Tregs of $S7^{\Delta DC}$ ($n = 8$) and control mice ($n = 7$) at the peak of disease (day 15; *Middle* and *Lower*, respectively). One representative of four independent experiments is depicted. Bar graphs depict mean value ± SEM. Statistical significance was assessed by using (*A*) EAE AUC followed by Student's *t* test and (*B–D*) Student's *t* test (*$P \leq 0.05$, **$P \leq 0.005$, and ***$P \leq 0.0005$).

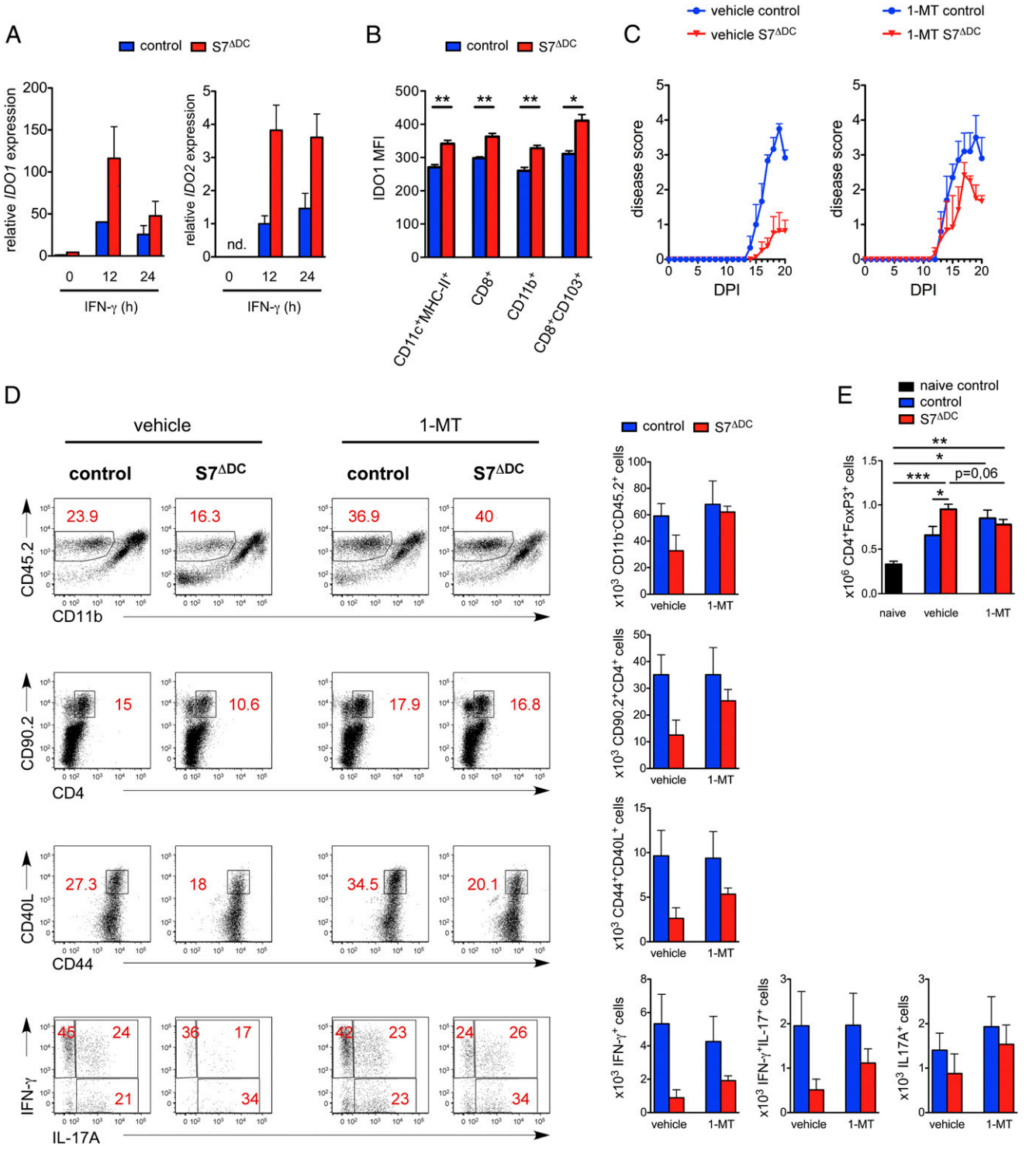


**Fig. 4.** Inhibition of IDO by 1-MT restores susceptibility of S7$^{\Delta DC}$ mice to EAE. (*A*) Relative expression of IDO1 and IDO2 in purified splenic CD11c$^+$ DCs isolated from S7$^{\Delta DC}$ ($n = 2$) and control mice ($n = 2$) left untreated or stimulated for 12 h or 24 h with 10 ng/mL IFN-γ. IDO1 and IDO2 expression levels were normalized to the respective controls. (*B*) IDO1 (MFI) of iLN-derived CD11c$^+$MHC-II$^+$, CD11c$^+$MHCII$^+$CD8$^+$, CD11c$^+$MHC-II$^+$CD11b$^+$, and CD11c$^+$MHC-II$^+$CD8$^+$CD103$^+$ DCs pregated on viable CD90.2$^-$B220$^-$ cells of control ($n = 4$) and S7$^{\Delta DC}$ ($n = 4$) mice on day 5 after EAE induction. (*C*) EAE disease progression in vehicle-treated control ($n = 3$) and S7$^{\Delta DC}$ ($n = 4$) mice and 1-MT–treated control ($n = 5$) and S7$^{\Delta DC}$ ($n = 3$) mice. Vehicle or 1-MT treatment was performed once on the day of $MOG_{35–55}$/CFA immunization. One representative of two independent experiments is shown. (*D*) Analysis of CNS infiltrates on day 20 after EAE induction in mice treated with vehicle or 1-MT from *B*. FACS blots illustrating CNS-infiltrating CD45.2$^+$CD11b$^-$ lymphocytes pregated on viable cells (*Upper*), CD90.2$^+$CD4$^+$ cells pregated on viable cells (*Upper Middle*), MOG-specific CD40L$^+$CD44$^+$ effector T cells pregated on viable CD90.2$^+$CD4$^+$ cells (*Lower Middle*), and MOG-specific Th1, Th17, and IL-17A$^+$IFNγ$^+$ double-producing cells as gated on viable CD90.2$^+$CD4$^+$CD40L$^+$CD44$^+$ cells (*Lower*). (*E*) Analysis of CD4$^+$FoxP3$^+$ Treg numbers in LNs from naïve control mice ($n = 3$) as well as EAE-immunized mice 10 d after immunization treated with vehicle [control ($n = 8$); S7$^{\Delta DC}$ ($n = 8$)] or 1-MT [control ($n = 5$); S7$^{\Delta DC}$ ($n = 6$)] on the day of EAE immunization. Cells were gated on viable CD90.2$^+$CD4$^+$ cells. (*A*, *B*, *D* and *E*) One experiment is depicted. Bar graphs represent mean value ± SEM. Statistical significance was assessed by Student's *t* test (*A*, *B*, and *E*), EAE AUC followed by two-way ANOVA and Bonferroni posttests (*C*), or two-way ANOVA and Bonferroni posttests (*D*) (*$P \leq 0.05$, **$P \leq 0.005$, and ***$P \leq 0.0005$).

(MFI; Fig. S3*C*). These findings were further confirmed by using GM-CSF–derived bone marrow DCs (BMDCs), left untreated or treated with LPS, in which MHC-II, CD80, CD86, and CD40 expression levels were comparable to those in controls (Fig. S3*D*). Moreover, 8 d after $MOG_{35–55}$/CFA and pertussis toxin (PTX) immunization, we did not observe any differences in T-cell activation, as frequencies and total cell counts of $CD62L^{-}CD44^{+}CD4^{+}$ T cells in spleen and inguinal LNs were similar to those in controls (Fig. S4*A*). Hence, Smad7-deficient DCs displayed a comparable ability to induce MOG-specific T-cell proliferation as determined by in vitro coculture of carboxyfluorescein succinimidyl ester (CFSE)-labeled 2D2 T cells with splenic DCs (Fig. S4*B*) or GM-CSF–derived BMDCs (Fig. S4*C*) from $S7^{\Delta DC}$ mice or controls. Similarly, Smad7-deficient DCs polarized naïve T cells toward Th1 and Th17 cells to the same extent as control DCs when using $MOG_{35–55}$–pulsed splenic DCs or BMDCs and naïve 2D2 T-cell cocultures (Fig. S5). Taken together, we found that loss of Smad7 does not alter DC antigen presentation, T-cell activation, and Th1/Th17 differentiation but rather promotes Treg development during EAE.

**Elevated Expression of IDO by Smad7-Deficient DCs Sustains Resistance to EAE.** To understand why $S7^{\Delta DC}$ mice exhibit increased numbers of Tregs during EAE, we purified $CD11c^{+}$ splenic DCs and analyzed their mRNA expression of *Ido1* and *Ido2* after in vitro stimulation with IFN-γ (19). We found that, upon IFN-γ exposure, DCs devoid of Smad7 showed increased *Ido1* and *Ido2* mRNA expression compared with control cells (Fig. 4*A*). Next, we investigated whether Smad7-deficient DCs also express higher IDO protein levels during EAE. Analysis of inguinal LN of $S7^{\Delta DC}$ mice 5 d after EAE induction revealed significantly increased IDO1 expression in all DC populations investigated, including $CD8^{+}$, $CD11b^{+}$, and $CD8^{+}CD103^{+}$ DC subsets compared with controls (Fig. 4*B*). To investigate whether IDO production by Smad7-deficient DCs was responsible for disease protection, we inhibited IDO activity by treatment with 1-methyl-D-tryptophan (1-MT). As depicted in Fig. 4*C*, 1-MT treatment as of the day of immunization restored disease susceptibility of $S7^{\Delta DC}$ mice to comparable levels as seen in 1-MT–treated controls (see also Fig. S6). Analysis of the CNS infiltrates in vehicle and 1-MT–treated mice confirmed that IDO inhibition also largely restored the numbers of encephalitogenic Th1, Th17, and $IL\text{-}17A^{+}IFN\text{-}\gamma^{+}$ double-producing MOG-specific effector $CD4^{+}$ T cells in the CNS of $S7^{\Delta DC}$ mice (Fig. 4*D*). In addition, when we analyzed inguinal LNs of $S7^{\Delta DC}$ mice 10 d after EAE immunization, a time point at which Treg cells in response to $MOG_{35–55}$/CFA are augmented, we noted that 1-MT treatment quenched the elevated number of Tregs detected in $S7^{\Delta DC}$ mice to comparable amounts as in 1-MT–treated controls (Fig. 4*E*). Taken together, these results strongly suggest that augmented IDO expression by Smad7-deficient DCs contributes to the higher Treg numbers and hence plays a prominent role in the reduced susceptibility to EAE observed in $S7^{\Delta DC}$ mice.

**EAE Resistance of $S7^{\Delta DC}$ Mice Is Caused by Elevated Amounts of Tregs.** Increased levels of IDO might not only affect Treg cell generation but, at the same time, also suppress effector T-cell differentiation. To discriminate the relative contribution of Tregs to disease outcome, $S7^{\Delta DC}$ mice were treated with an anti-CD25 depleting antibody (PC61) or with an isotype control antibody before disease induction (Fig. 5*A*). As expected, control antibody treatment did not change the course of disease in WT, and $S7^{\Delta DC}$ mice retain their resistance (Fig. 5*A*, *Left*). In contrast, when injected with PC61, WT mice developed exacerbated disease, with approximately two times higher mean clinical scores compared with control antibody-treated mice (Fig. 5*A*, *Left* and *Right*). Furthermore, PC61-treated WT mice failed to resolve EAE, unlike WT controls. Intriguingly, Treg depletion rendered $S7^{\Delta DC}$ mice susceptible to severe EAE. Disease progression of PC61-treated $S7^{\Delta DC}$ and WT mice was characterized by comparable mean clinical scores and similar lack of EAE remission (Fig. 5*A*, *Right*). Further histological examination confirmed that PC61-treated $S7^{\Delta DC}$ mice suffer from CNS inflammation, as documented by demyelination ($LFB\text{-}PAS^{+}$ cells), infiltration of $CD3^{+}$ T cells, $MAC3^{+}$ macrophages, $B220^{+}$ B cells, and visible axonal damage [i.e., amyloid precursor protein-expressing ($APP^{+}$) cells; Fig. 5*B*].

**EAE Resistance of $S7^{\Delta DC}$ Mice Is Dependent on Intact IFN-γ Signaling.** DC-specific absence of Smad7 resulted in reduced EAE susceptibility, which was mediated by increased IDO levels driving the induction of more protective Tregs. As IDO expression in DCs is triggered upon IFN-γ signaling, we analyzed whether signaling to this cytokine might be responsible for the elevated IDO levels and the resistance of $S7^{\Delta DC}$ mice to EAE. Therefore, $S7^{\Delta DC}$ mice were crossed to animals that allow the conditional deletion of the IFN-γ receptor 2 (IFN-γR2), resulting in mice that lack Smad7 and IFN-γ signaling specifically in DCs ($IFN\text{-}\gamma R2^{\Delta DC}S7^{\Delta DC}$ mice). As depicted in Fig. 6, simultaneous deletion of IFN-γ signaling and Smad7 in DCs restored EAE susceptibility of $S7^{\Delta DC}$ mice, whereas $IFN\text{-}\gamma R2^{\Delta DC}S7^{+/-\Delta DC}$ mice developed disease similar to WT controls. These data suggest that Smad7 regulates IDO expression in DCs when exposed to IFN-γ in vivo and that resistance of $S7^{\Delta DC}$ mice to EAE is mainly driven by uncontrolled IFN-γ–mediated IDO expression in DCs.

In conclusion, our data establish a critical role for Smad7 during the differentiation of $IDO^{+}$ tolerogenic DCs during inflammation and its physiological relevance in Treg-mediated tolerance of autoimmune inflammation.

## Discussion

Studies using genetically modified mice established a prominent role for TGF-β in anti-inflammatory responses important for the maintenance of immune homeostasis and the establishment of tolerance (1–5), including the observation that TGF-β signaling in DCs is a prerequisite for the control of EAE (23). On the contrary, little is known about the function of the TGF-β–negative regulator Smad7 in DCs. By using mice with a DC-specific deletion of Smad7 ($S7^{\Delta DC}$), we characterized the role of Smad7 during DC homeostasis and function, particularly its impact on the outcome of CNS autoimmunity. Except for an increase in $CD8^{+}CD103^{+}$ DCs in the spleen, we did not observe any other obvious differences between $S7^{\Delta DC}$ and control animals under steady-state conditions. When stimulated with IFN-γ or TGF-β, Smad7-deficient DCs expressed elevated levels of the transcription factors IRF8 and Batf3. Following IFN-γ stimulation, loss of Smad7 led to higher IDO production by DCs and, consequently (19), an increased percentage and absolute number of Tregs in vivo. In line, $S7^{\Delta DC}$ mice were resistant to the induction of EAE by MOG immunization and did display only minor signs of CNS demyelination compared with control animals.

In the steady state, DC-specific Smad7 deletion resulted in a shift in splenic DC populations toward the differentiation of $CD8^{+}CD103^{+}$ DCs. This bias was mediated by increased expression of the corresponding lineage-defining transcription factors Batf3 and IRF8. Previously, it was shown that the stimulation of murine DC progenitor cells with TGF-β led to increased development of conventional DCs at the expense of pDCs (33). However, the resulting conventional DC subsets and their function were not further analyzed in this study. Development of $CD8^{+}$ and $CD103^{+}$ DCs is dependent on the transcription factors IRF8 and Batf3 (12, 13). To date, the mediators that induce these transcription factors during DC differentiation remain poorly defined. As $S7^{\Delta DC}$ mice displayed increased frequencies of splenic $CD8^{+}CD103^{+}$ DCs associated with elevated expression of IRF8 and Batf3, our data suggest that Smad7 negatively influences expression of $CD8^{+}CD103^{+}$ lineage-defining transcription factors in response to TGF-β. This conclusion is supported by a previous publication in which blockade of the TGF-β pathway by ectopic

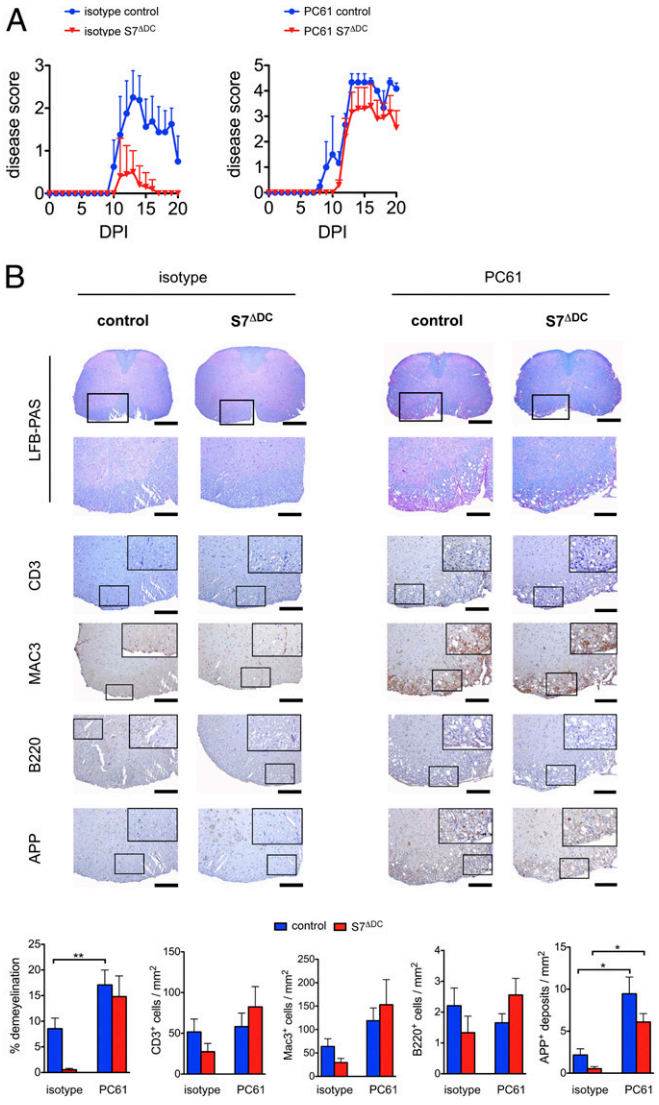


**Fig. 5.** Deletion of Treg cells in S7$^{\Delta DC}$ mice reverses EAE resistance. (*A*) EAE disease scores of isotype-treated (*Left*) or PC61-treated (*Right*) S7$^{\Delta DC}$ ($n$ = 5 and $n$ = 4, respectively) and control mice ($n$ = 5 and $n$ = 4, respectively). Shown is one representative of two independent experiments. (*B*) Histological quantification of spinal cords 23 d after EAE induction from S7$^{\Delta DC}$ ($n$ = 5–4) or control mice ($n$ = 5–4) treated with isotype or PC61 as seen in *A*. Spinal cord sections were stained with Luxol fast blue/periodic acid-Schiff (LFB-PAS) to reveal the degree of demyelination, for CD3$^+$ infiltrates, Mac3$^+$ and B220$^+$ infiltrates, and APP$^+$ deposits exposing axonal damage as indicated. Respective infiltrating cells/deposits were calculated per squared millimeter. (Scale bar: 50 μm.) Bar graphs depict mean value ± SEM. Statistical significance was assessed by EAE AUC followed by two-way ANOVA and Bonferroni posttests (*A*) and two-way ANOVA and Bonferroni posttests (*B*) (*$P \leq 0.05$, **$P \leq 0.005$, and ***$P \leq 0.0005$).

expression of Smad7 abolished the up-regulation of IRF8, which indicates a direct role for Smad7 in IRF8 repression (29). Smad7 is able to bind DNA through its MH2 domain (34, 35) and to associate with the histone deacetylases HDAC1 and SIRT1, thus regulating transcription by repressing promoter activity (36–38). However, whether Smad7 affects CD8$^+$CD103$^+$ DC differentiation by direct repression of IRF8 and Batf3 promoter activity or regulates another unknown factor(s) controlling Batf3 and IRF8 expression remains elusive. Although pDC development is likewise dependent on IRF8, the percentages and absolute numbers of pDCs in S7$^{\Delta DC}$ mice remained unchanged. Although CD11c-Cre mice can effectively target all DC subsets, including pDCs (25), the efficiency of Cre-mediated recombination also depends on the accessibility of the target gene, as we have recently revealed that pDCs were not depleted by using the inducible diphtheria toxin receptor (iDTR) system when targeted by the same CD11c-Cre (22). Alternatively, it is conceivable that other molecules besides Smad7 control IRF8 expression in pDCs.

Steady-state expression of MHC-II and costimulatory molecules was not affected by deletion of Smad7. Hence, T-cell homeostasis and activation were unchanged in S7$^{\Delta DC}$ mice, including similar numbers of Tregs despite the increased frequency of splenic CD8$^+$CD103$^+$ DCs. In contrast, when subjected to EAE, S7$^{\Delta DC}$ mice displayed significantly milder disease progression accompanied by elevated numbers of CNS-infiltrating Tregs and reduced numbers of MOG-reactive effector T cells based on CD40L expression upon MOG restimulation of CNS-infiltrating lymphocytes (22, 32). Because lack of Smad7 also did not affect DC maturation, i.e., antigen presentation or costimulation, these data strongly suggest that, upon EAE induction, absence of Smad7 in DCs led to augmented numbers of Tregs, which in turn suppressed differentiation of encephalitogenic effector T cells. In line with this, abrogated TGF-β receptor signaling in DCs resulted in severe EAE (23) and spontaneous multiorgan autoimmune disease with increasing age (18), indicating that TGF-β signaling is critical for the suppressive function of the DC. However, these studies did not detect differences in the development of DC subpopulations or in IDO expression. It was recently demonstrated that absent TGF-β signaling in mature CD4$^+$ T cells does not lead to breakdown of peripheral tolerance (39), thus suggesting that TGF-β signaling in DCs and not in T cells is mandatory for peripheral tolerance. On the contrary, mice with a T-cell–specific deletion of Smad7 are resistant to the induction of EAE (24). Our new findings support a critical role of Smad7 as an inhibitor of a tolerogenic DC phenotype. In particular, CD8$^+$CD103$^+$ DCs have been previously linked to tolerance induction in part as a result of increased IDO expression, which mediates enhanced Treg differentiation upon challenge (16, 19, 40–42). In agreement with the requirement of a proinflammatory stimulus, in our study, all conventional DC subsets devoid of Smad7 exhibited elevated IDO expression following IFN-γ stimulation in vitro and during EAE. Indeed, IDO plays a prominent role in MS and during EAE, as increased IDO protein levels are detected in the CNS and peripheral organs during these diseases (43–46). By using IDO$^{-/-}$ mice, it was shown that IDO augments Tregs via tryptophan metabolites and suppresses encephalitogenic T-cell responses in EAE (20). IDO expression is induced upon TGF-β as well as IFN-γ signaling (19, 40), and likewise IFNγR$^{-/-}$ mice lack IDO activity (47). Hence, during EAE, IDO might be produced in response to IFN-γ and contributes to terminate inflammation in a negative feedback loop (43–46). However, most studies addressing the tolerogenic function of IDO used models of global overexpression or inhibition of IDO. Here, we provide evidence that, upon inflammation, DC-specific IDO expression supports Treg-mediated tolerance and that Smad7 controls this tolerogenic DC phenotype. Moreover, our data suggest that this IDO-mediated resistance to EAE, observed in S7$^{\Delta DC}$ mice, is dependent on IFN-γ signaling as DC-specific ablation of IFN-γR2 and Smad7 resulted in normal disease development.

Although IFN-γ was originally described as a proinflammatory cytokine, as its expression was associated with pathogenic Th1 cells, more recently it became evident that IFN-γ actually ameliorates EAE disease progression (42, 48–51). Moreover, the tolerogenic function of IFN-γ is not limited to EAE but similarly applies to other autoimmune diseases such as autoimmune myocarditis (52) and collagen-induced arthritis (53, 54). Our data indicate that Smad7 expression in DCs in response to IFN-γ during inflammation would not only inhibit TGF-β signaling but, at the same time, suppress expression of the transcription factor IRF8 that is important for IDO induction. Abrogated IDO expression in mice

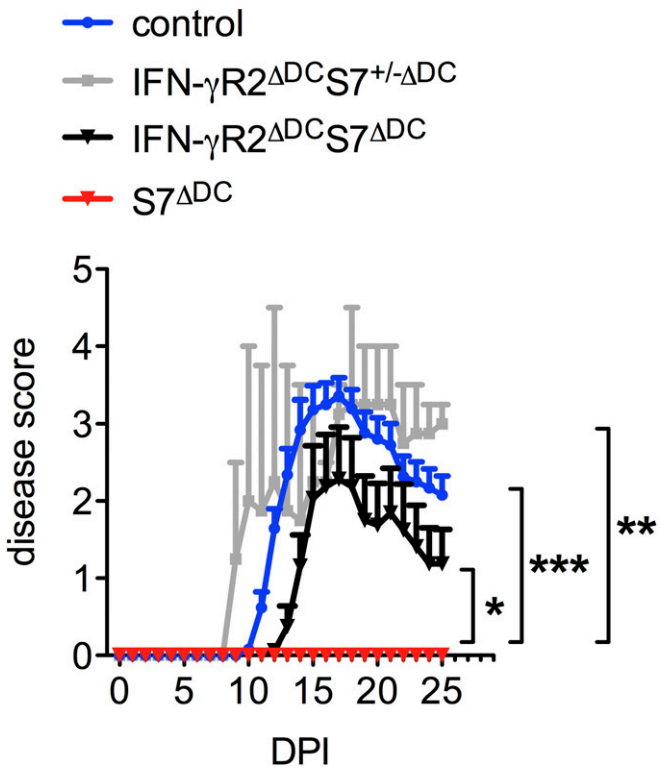


**Fig. 6.** DC-specific ablation of IFN-γR2 restores susceptibility of $S7^{\Delta DC}$ mice to EAE. Disease scores of WT control ($n = 19$), $S7^{\Delta DC}$ ($n = 4$), IFN-γ$R2^{\Delta DC}S7^{+/-\Delta DC}$ ($n = 2$), and IFN-γ$R2^{\Delta DC}S7^{\Delta DC}$ ($n = 8$) mice subjected to EAE are shown. Graph represents mean value ± SEM. One representative of two independent experiments is depicted. Statistical significance was assessed by using AUC followed by one-way ANOVA and Newman–Keuls multiple comparison test (*$P \leq 0.05$, **$P \leq 0.005$, and ***$P \leq 0.0005$).

with DCs lacking the IFN-γR2 and Smad7 in turn results in reduced Treg differentiation and consequently susceptibility to EAE.

In the time course analyzed here, we did not observe a difference in EAE between controls and mice with DC-specific IFN-γR2 deficiency alone. This may indicate that, under strong inflammatory conditions in acute EAE, the effect of IFN-γ–mediated IDO expression and Treg induction may be well counterbalanced by Smad7 and inflammatory cytokines such as IL-6 and IL-1β.

Given that Smad7 in DCs represents a key molecular switch that regulates IDO expression during ongoing inflammation, Smad7 inhibition may provide a promising therapeutic approach for the treatment of chronic inflammatory diseases. Indeed, Smad7 antisense oligonucleotide therapy suppressed EAE (55) and experimental colitis in mice (56) and is currently being tested in a phase III clinical trial with promising prospects in patients with Crohn's disease (ref. 57; www.clinicaltrials.gov: NCT02596893). In addition, simvastatin efficiently abrogates Smad7, resulting in a higher frequency of $FoxP3^+$ Tregs in mice (58). Notably, none of these drugs were cell type-specific. Based on our findings, a Smad7 inhibitor should offer an attractive approach to treat autoimmune patients while minimizing potential adverse side effects.

In conclusion, in this study, we have identified a crucial role for Smad7 in DC differentiation and function. In the steady state, Smad7 regulates the expression of the transcription factors Batf3 and IRF8 that promote the development of $CD8^+CD103^+$ DCs in the spleen. During inflammation, Smad7 governs the tolerogenic function of conventional DCs by regulating IDO-mediated Treg induction. Hence, DC-specific Smad7 deletion alleviates EAE, which may be exploited for therapy of autoimmune diseases.

## Materials and Methods

**Mice.** CD11c-$Cre^{+/-}$ mice (25) were bred to $Smad7^{fl/fl}$ mice (24) to generate animals with a DC-specific Smad7 deletion ($S7^{\Delta DC}$). Cre-negative littermates or C57BL/6 WT mice were used as controls. In addition, $S7^{\Delta DC}$ mice were bred to IFN-γ$RII^{fl/fl}$ mice (59), resulting in a mouse line with DC-specific loss of Smad7 and IFN-γRII (IFN-γ$R2^{\Delta DC}S7^{\Delta DC}$). All animals were on a C57BL/6 background and kept under specific pathogen-free conditions at the central animal facility in Mainz. Experiments were performed in accordance with guidelines of the institutional animal care and use committee of the University of Mainz.

**Induction and Clinical Evaluation of EAE.** Eight- to 10-wk-old mice were injected with 50 μg $MOG_{35-55}$ in CFA containing 8 mg/mL concentration of heat-inactivated *Mycobacterium tuberculosis* H37RA (Difco Laboratories) into the tail base. On days 0 and 2, mice were injected intraperitoneally with 200 ng pertussis toxin (Sigma-Aldrich). Daily scoring was performed using the following criteria: 0, healthy; 1, limp tail; 2, partial hindlimb weakness/ataxia; 3, paralysis of at least one hindlimb; 4, complete hindlimb paralysis; 5, partial forelimb paralysis; and 6, moribund/dead.

**In Vivo Inhibition of IDO Activity Using 1-MT.** Mice were treated with 10 mg 1-MT (Sigma-Aldrich) reconstituted in 2 M HCl and adjusted to pH 7 using 2 M NaOH or were injected with the respective vehicle control on the day of $MOG_{35/55}$/CFA immunization.

**In Vivo Depletion of $CD25^+$ Cells.** Mice were treated with 0.5 mg PC61 (αCD25 antibody; BioXcell) or 0.5 mg IgG1 isotype control (BioXcell) at 5 and 3 d before $MOG_{35-55}$/CFA immunization. To test for efficient cell depletion, mice were bled 1 d before $MOG_{35-55}$/CFA immunization, and circulating leukocytes were stained for surface CD25 expression.

**Lymphoid Tissue Preparation.** Thymi, spleens, and LNs were harvested from $S7^{\Delta DC}$ and control mice and homogenized in ice-cold PBS solution ($-Ca^{2+}/-Mg^{2+}$; Gibco) containing 2% (vol/vol) FCS using 40-μm cell strainers (BD Biosciences). For preparation of DCs, lymphoid tissues were preincubated with 2 mg/mL collagenase type II (Gibco) and 20 U of DNaseI (Sigma-Aldrich) at 37 °C. Cell counts were determined by using a Neubauer chamber or CASYton cell counter (Roche Applied Science).

**CNS Isolation.** Mice were anesthetized and perfused with ice-cold PBS solution. Brain and spinal cords were removed and homogenized by using a razor blade. Tissue was incubated for 30 min with PBS solution ($+Ca^{2+}/+Mg^{2+}$) containing 2 mg/mL collagenase type II and 20 U of DNaseI at 37 °C. The tissue was then homogenized with a syringe, and CNS-infiltrating cells were isolated on a Percoll gradient [containing 30, 37, and 70% (vol/vol) Percoll] (60).

**Antigen Uptake.** Mice were injected s.c. with 50 μL per mouse of 1.0-μm Fluoresbrite YG Microspheres (Polysciences) emulsified in $MOG_{35/55}$/CFA. Antigen uptake and DC migration was assessed 24 h, 48 h, and 72 h later by analysis of fluorescently labeled cells found in the dLN.

**BMDC Culture.** For preparation of BMDCs, mice were killed and BM cells were flushed out of the femurs. A total of $2 \times 10^6$ cells per milliliter were incubated for at least 8 d in Iscove's modified Dulbecco's medium containing 5% (vol/vol) GM-CSF, 10% (vol/vol) FCS, 50 mM β–mercaptoethanol, 2 mM glutamine, and 100 units/mL penicillin, 100 mg/mL streptomycin. Maturation of BMDCs was achieved by stimulation of the cells with 1μg/mL LPS for 24 h. Harvesting of DCs was performed by incubation of the cells with trypsin (Gibco) for 5 min.

**DC/T-Cell Coculture.** A total of $0.5 \times 10^6$ CFSE-labeled MACS-purified $2D2^+$ $MOG_{35-55}$–specific $CD4^+$ T cells were cocultured with MACS-purified DCs isolated from collagenase-treated spleens. DC/T cells were cultured in a ratio of 1:10 or 1:20 in Roswell Park Memorial Institute (RPMI) medium (supplemented with 2 mM glutamine, 100 units/mL penicillin, 100 mg/mL streptomycin, 50 mM β–mercaptoethanol, and 1 or 5 μg/mL $MOG_{35-55}$). Cells were cultured in round-bottom 96-well plates in the absence or presence of 10 ng/mL TGF-β for 4–5 d at 37 °C and 5% $CO_2$.

**In Vitro DC-Mediated Th1 and Th17 Cell Differentiation.** A total of 40,000 DCs derived from spleen and LN, enriched by using Dynabeads Mouse DC enrichment kit (Invitrogen), were cocultured with 400,000 $CD4^+CD62L^+$ MACS-purified naïve 2D2 T cells for 6 d in RPMI media (supplemented with 10% (vol/vol) FCS, 2 mM glutamine, 100 units/mL penicillin, 100 mg/mL streptomycin,

and 50 mM β-mercaptoethanol) containing medium alone or medium supplemented with 20 μg/mL $MOG_{35–55}$ with or without 1 μg/mL LPS and in the presence or absence of 10 ng/mL TGF-β.

A total of 20,000 GM-CSF–derived BMDCs were cocultured with 400,000 $CD4^+CD62L^+$ MACS-purified naïve 2D2 T cells for 6 d in RPMI media [supplemented with 10% (vol/vol) FCS, 2 mM glutamine, 100 units/mL penicillin, 100 mg/mL streptomycin, and 50 mM β-mercaptoethanol] containing medium alone or medium supplemented with 20 μg/mL $MOG_{35–55}$ with or without 1 μg/mL LPS and in the presence or absence of 10 ng/mL TGF-β.

**Flow Cytometry.** The following antibodies were purchased from BD Biosciences unless otherwise specified: anti-mouse CD4 (L3T4), CD8α (53-6.7), CD11b (M1/70), CD19 (1D3), CD25 (7D4), CD44 (IM7), CD45.2 (104), CD62L (MEL-14), CD69 (H1.2F3), CD90.2 (53-2.1), CD11c (HL3), Siglec-H (eBio440c; eBiosciences), MHC-II (M5/114; eBiosciences), CD40 (3/23), CD80 (16-10A1), CD86 (GL1; eBiosciences), CD90.1 (OX-7), CD90.2 (53-201; eBiosciences), B220 (RA3-6B2; BioLegend), CD103 (M290; BioLegend), CD154 (MR-1; BioLegend, eBiosciences), and PDL1 (MIH5; eBiosciences).

Intracellular staining for IL-17A, IFN-γ and IDO1 was performed after cell restimulation for 4 h with 50 ng/mL phorbol 12-myristate 13-acetate, 500 ng/mL ionomycin, and 5 mg/mL brefeldin A. For discrimination of $MOG_{35–55}$–specific effector T cells, cells were stimulated with 20 μg/mL $MOG_{35–55}$ for 3 h, and then 5 mg/mL brefeldin A was added, and cells were cultured for an additional 3 h. Antibodies specific for mouse IL-17A (clone TC11-18H10.1), IFN-γ (clone XMG1.2), Foxp3 (clone FJK-16s; eBioscience), and IDO1 (clone 2E2.6; Novus Biologicals) were used for intracellular cytokine staining. Intracellular stainings were performed according to the protocol of the BD Cytofix/Cytoperm kit (BD Biosciences) or Foxp3/Transcription Factor Staining Buffer set (eBiosciences). Cells were analyzed by using a FACSCanto device (BD Biosciences) with FACSDiva software (BD Biosciences) or FACScan (BD Biosciences) with CellQuest (BD Biosciences) software. Postacquisition analysis was performed by using FlowJo or CellQuest software.

**Immunohistochemistry.** Histology was performed as described previously (61). Mice were perfused during deep anesthesia with ice-cold saline solution. Spinal cords were removed and fixed in 4% (vol/vol) buffered formalin. Then, spinal cords were dissected and embedded in paraffin before staining with H&E, Luxol fast blue to assess the degree of demyelination, macrophage-3 antigen (clone M3/84, dilution 1:200; BD Pharmingen) for macrophages/microglia, CD3 for T cells (clone CD3-12, dilution 1:100; Serotec), B220 for B cells (clone RA3-6B2, dilution 1:200; BD Pharmingen), and deposition of APP (clone 22C11, dilution 1:3,000; Millipore), which reflects axonal damage. Secondary antibodies were polyclonal rabbit anti-mouse biotinylated (E0464, lot 00073409; DAKO) and used in a dilution of 1:200, in combination with avidin-peroxidase (A7419, 1:1,000; Sigma-Aldrich). Tissue sections were evaluated on an Olympus BX-61 microscope with the use of cell-P software (Olympus).

**Quantitative Real-Time PCR.** Total mRNA was isolated by using the RNEasy kit (Qiagen) from MACS-purified $CD11c^+$ cells or Dynabeads DC-enriched splenic cells. cDNA preparation was performed by using SuperScript reverse transcriptase (Invitrogen). Quantitative real-time PCR of mRNA coding for Smad7, IRF8, Batf3, IDO1, and IDO2 was performed by using primers from Qiagen and the QuantiTect SYBR Green RT-PCR kit. The relative mRNA amounts were determined by normalization to the housekeeping genes GAPDH or hypoxanthine guanine phosphoribosyl transferase (HPRT). The expression levels of mRNA were calculated by using the $\Delta C_T$ method and normalized to the WT control.

**TGF-β Cytokine Bead Array.** For the measurement of TGF-β cytokine production, $0.5 \times 10^6$ DCs were stimulated with or without 1 μg/mL LPS (*Escherichia coli* 026.B6; Sigma-Aldrich) in RPMI [supplemented with 10% (vol/vol) FCS, 2 mM glutamine, 100 mg/mL streptomycin, 100 U/mL penicillin, and 5 mM β-mercaptoethanol] overnight. Supernatants were harvested, and cells were washed with PBS solution and stimulated with soluble CD40L (sCD40L; PeproTech) for an additional 24 h when supernatants were collected. The levels of TGF-β in supernatants of stimulated cells were determined by cytometric bead assay (Bender MedSystems) according to the manufacturer's instructions. Analysis was performed on a FACSCanto-II (BD Biosciences), and the concentration of measured cytokines was calculated by using FCAP Array software (BD Biosciences).

**Statistical Analysis.** Values are presented as mean ± SEM. Statistical significance between two groups was assessed by using two-tailed Student's *t* test. When comparing two groups with two additional treatments, two-way ANOVA and Bonferroni posttests were used. When comparing two EAE groups, statistical significance was determined by measurements of EAE area under the curve (AUC) followed by Student's *t* test. EAE significance of two groups with two different treatments was assessed by measurement of EAE AUC followed by two-way ANOVA and Bonferroni posttests. $P > 0.05$ was considered not significant.

**ACKNOWLEDGMENTS.** We thank Marina Snetkova, Alexei Nikolaev, Michaela Blanfeld, Petra Adams-Quack, Lara Jungmann, and Maria Oberle for their excellent technical assistance; and Maja Kitic and Julia Ober-Blöbaum for their comments, help, and advice. This work was supported by Deutsche Forschungsgemeinschaft Grants TRR128 TP A07 (to A.W.), WA1600/8-1 (to A.W.), and KL2187/1-1 (to I.K.); the Gemeinnützige Hertie-Stiftung (A.W. and B.E.C.); and the Netherlands Organization for Scientific Research (NWO) Grant VIDI 917-76-365 (to B.E.C.). B.E.C. and A.W. are members of the Research Center for Immunotherapy Mainz, and A.W. is a member of the Focus Program Translational Neuroscience.

1. Kulkarni AB, et al. (1993) Transforming growth factor beta 1 null mutation in mice causes excessive inflammatory response and early death. *Proc Natl Acad Sci USA* 90(2): 770–774.
2. Shull MM, et al. (1992) Targeted disruption of the mouse transforming growth factor-beta 1 gene results in multifocal inflammatory disease. *Nature* 359(6397): 693–699.
3. Dang H, et al. (1995) SLE-like autoantibodies and Sjögren's syndrome-like lymphoproliferation in TGF-beta knockout mice. *J Immunol* 155(6):3205–3212.
4. Yaswen L, et al. (1996) Autoimmune manifestations in the transforming growth factor-beta 1 knockout mouse. *Blood* 87(4):1439–1445.
5. Li MO, Sanjabi S, Flavell RA (2006) Transforming growth factor-beta controls development, homeostasis, and tolerance of T cells by regulatory T cell-dependent and -independent mechanisms. *Immunity* 25(3):455–471.
6. Yan X, Chen YG (2011) Smad7: Not only a regulator, but also a cross-talk mediator of TGF-β signalling. *Biochem J* 434(1):1–10.
7. Ulloa L, Doody J, Massagué J (1999) Inhibition of transforming growth factor-beta/SMAD signalling by the interferon-gamma/STAT pathway. *Nature* 397(6721):710–713.
8. Steinman RM, et al. (2003) Dendritic cell function in vivo during the steady state: A role in peripheral tolerance. *Ann N Y Acad Sci* 987:15–25.
9. Steinman RM, Hawiger D, Nussenzweig MC (2003) Tolerogenic dendritic cells. *Annu Rev Immunol* 21:685–711.
10. Belz GT, Nutt SL (2012) Transcriptional programming of the dendritic cell network. *Nat Rev Immunol* 12(2):101–113.
11. Merad M, Sathe P, Helft J, Miller J, Mortha A (2013) The dendritic cell lineage: Ontogeny and function of dendritic cells and their subsets in the steady state and the inflamed setting. *Annu Rev Immunol* 31:563–604.
12. Hildner K, et al. (2008) Batf3 deficiency reveals a critical role for CD8alpha+ dendritic cells in cytotoxic T cell immunity. *Science* 322(5904):1097–1100.
13. Tailor P, Tamura T, Morse HC, 3rd, Ozato K (2008) The BXH2 mutation in IRF8 differentially impairs dendritic cell subset development in the mouse. *Blood* 111(4): 1942–1945.
14. Perry JS, et al. (2014) Distinct contributions of Aire and antigen-presenting-cell subsets to the generation of self-tolerance in the thymus. *Immunity* 41(3):414–426.
15. Coombes JL, et al. (2007) A functionally specialized population of mucosal CD103+ DCs induces Foxp3+ regulatory T cells via a TGF-beta and retinoic acid-dependent mechanism. *J Exp Med* 204(8):1757–1764.
16. Yamazaki S, et al. (2008) CD8+ CD205+ splenic dendritic cells are specialized to induce Foxp3+ regulatory T cells. *J Immunol* 181(10):6923–6933.
17. Yamaguchi Y, Tsumura H, Miwa M, Inaba K (1997) Contrasting effects of TGF-beta 1 and TNF-alpha on the development of dendritic cells from progenitors in mouse bone marrow. *Stem Cells* 15(2):144–153.
18. Ramalingam R, et al. (2012) Dendritic cell-specific disruption of TGF-β receptor II leads to altered regulatory T cell phenotype and spontaneous multiorgan autoimmunity. *J Immunol* 189(8):3878–3893.
19. Pallotta MT, et al. (2011) Indoleamine 2,3-dioxygenase is a signaling protein in long-term tolerance by dendritic cells. *Nat Immunol* 12(9):870–878.
20. Yan Y, et al. (2010) IDO upregulates regulatory T cells via tryptophan catabolite and suppresses encephalitogenic T cell responses in experimental autoimmune encephalomyelitis. *J Immunol* 185(10):5953–5961.
21. Kurschus FC, Wörtge S, Waisman A (2011) Modeling a complex disease: Multiple sclerosis. *Adv Immunol* 110:111–137.
22. Yogev N, et al. (2012) Dendritic cells ameliorate autoimmunity in the CNS by controlling the homeostasis of PD-1 receptor(+) regulatory T cells. *Immunity* 37(2): 264–275.
23. Laouar Y, et al. (2008) TGF-beta signaling in dendritic cells is a prerequisite for the control of autoimmune encephalomyelitis. *Proc Natl Acad Sci USA* 105(31):10865–10870.

24. Kleiter I, et al. (2010) Smad7 in T cells drives T helper 1 responses in multiple sclerosis and experimental autoimmune encephalomyelitis. *Brain* 133(pt 4):1067–1081.
25. Caton ML, Smith-Raska MR, Reizis B (2007) Notch-RBP-J signaling controls the homeostasis of CD8- dendritic cells in the spleen. *J Exp Med* 204(7):1653–1664.
26. Hadley GA, Bartlett ST, Via CS, Rostapshova EA, Moainie S (1997) The epithelial cell-specific integrin, CD103 (alpha E integrin), defines a novel subset of alloreactive $CD8^+$ CTL. *J Immunol* 159(8):3748–3756.
27. Mokrani M, Klibi J, Bluteau D, Bismuth G, Mami-Chouaib F (2014) Smad and NFAT pathways cooperate to induce CD103 expression in human CD8 T lymphocytes. *J Immunol* 192(5):2471–2479.
28. El-Asady R, et al. (2005) TGF-beta-dependent CD103 expression by CD8(+) T cells promotes selective destruction of the host intestinal epithelium during graft-versus-host disease. *J Exp Med* 201(10):1647–1657.
29. Ju XS, et al. (2007) Transforming growth factor beta1 up-regulates interferon regulatory factor 8 during dendritic cell development. *Eur J Immunol* 37(5):1174–1183.
30. Politis AD, Sivo J, Driggers PH, Ozato K, Vogel SN (1992) Modulation of interferon consensus sequence binding protein mRNA in murine peritoneal macrophages. Induction by IFN-gamma and down-regulation by IFN-alpha, dexamethasone, and protein kinase inhibitors. *J Immunol* 148(3):801–807.
31. Kantakamalakul W, et al. (1999) Regulation of IFN consensus sequence binding protein expression in murine macrophages. *J Immunol* 162(12):7417–7425.
32. Chattopadhyay PK, Yu J, Roederer M (2005) A live-cell assay to detect antigen-specific $CD4^+$ T cells with diverse cytokine profiles. *Nat Med* 11(10):1113–1117.
33. Felker P, et al. (2010) TGF-beta1 accelerates dendritic cell differentiation from common dendritic cell progenitors and directs subset specification toward conventional dendritic cells. *J Immunol* 185(9):5326–5335.
34. Zhang S, et al. (2007) Smad7 antagonizes transforming growth factor beta signaling in the nucleus by interfering with functional Smad-DNA complex formation. *Mol Cell Biol* 27(12):4488–4499.
35. Shi X, et al. (2008) Study of interaction between Smad7 and DNA by single-molecule force spectroscopy. *Biochem Biophys Res Commun* 377(4):1284–1287.
36. Grönroos E, Hellman U, Heldin CH, Ericsson J (2002) Control of Smad7 stability by competition between acetylation and ubiquitination. *Mol Cell* 10(3):483–493.
37. Simonsson M, Heldin CH, Ericsson J, Grönroos E (2005) The balance between acetylation and deacetylation controls Smad7 stability. *J Biol Chem* 280(23):21797–21803.
38. Kume S, et al. (2007) SIRT1 inhibits transforming growth factor beta-induced apoptosis in glomerular mesangial cells via Smad7 deacetylation. *J Biol Chem* 282(1): 151–158.
39. Sledzińska A, et al. (2013) TGF-β signalling is required for $CD4^+$ T cell homeostasis but dispensable for regulatory T cell function. *PLoS Biol* 11(10):e1001674.
40. Belladonna ML, et al. (2008) Cutting edge: Autocrine TGF-beta sustains default tolerogenesis by IDO-competent dendritic cells. *J Immunol* 181(8):5194–5198.
41. Matteoli G, et al. (2010) Gut $CD103^+$ dendritic cells express indoleamine 2,3-dioxygenase which influences T regulatory/T effector cell balance and oral tolerance induction. *Gut* 59(5):595–604.
42. Pettersson A, et al. (2004) CD8alpha dendritic cells and immune protection from experimental allergic encephalomyelitis. *Clin Exp Immunol* 137(3):486–495.
43. Sakurai K, Zou JP, Tschetter JR, Ward JM, Shearer GM (2002) Effect of indoleamine 2,3-dioxygenase on induction of experimental autoimmune encephalomyelitis. *J Neuroimmunol* 129(1-2):186–196.
44. Kwidzinski E, et al. (2005) Indolamine 2,3-dioxygenase is expressed in the CNS and down-regulates autoimmune inflammation. *FASEB J* 19(10):1347–1349.
45. Kwidzinski E, et al. (2003) IDO (indolamine 2,3-dioxygenase) expression and function in the CNS. *Adv Exp Med Biol* 527:113–118.
46. Orsini H, et al. (2014) GCN2 kinase plays an important role triggering the remission phase of experimental autoimmune encephalomyelitis (EAE) in mice. *Brain Behav Immun* 37:177–186.
47. O'Connor JC, et al. (2009) Interferon-gamma and tumor necrosis factor-alpha mediate the upregulation of indoleamine 2,3-dioxygenase and the induction of depressive-like behavior in mice in response to bacillus Calmette-Guerin. *J Neurosci* 29(13): 4200–4209.
48. Willenborg DO, Fordham SA, Staykova MA, Ramshaw IA, Cowden WB (1999) IFN-gamma is critical to the control of murine autoimmune encephalomyelitis and regulates both in the periphery and in the target tissue: A possible role for nitric oxide. *J Immunol* 163(10):5278–5286.
49. Chu CQ, Wittmer S, Dalton DK (2000) Failure to suppress the expansion of the activated CD4 T cell population in interferon gamma-deficient mice leads to exacerbation of experimental autoimmune encephalomyelitis. *J Exp Med* 192(1):123–128.
50. Tran EH, Prince EN, Owens T (2000) IFN-gamma shapes immune invasion of the central nervous system via regulation of chemokines. *J Immunol* 164(5):2759–2768.
51. Weishaupt A, et al. (2000) Molecular mechanisms of high-dose antigen therapy in experimental autoimmune encephalomyelitis: Rapid induction of Th1-type cytokines and inducible nitric oxide synthase. *J Immunol* 165(12):7157–7163.
52. Eriksson U, et al. (2001) Lethal autoimmune myocarditis in interferon-gamma receptor-deficient mice: Enhanced disease severity by impaired inducible nitric oxide synthase induction. *Circulation* 103(1):18–21.
53. Vermeire K, Thielemans L, Matthys P, Billiau A (2000) The effects of NO synthase inhibitors on murine collagen-induced arthritis do not support a role of NO in the protective effect of IFN-gamma. *J Leukoc Biol* 68(1):119–124.
54. Chong WP, et al. (2015) NK-DC crosstalk controls the autopathogenic Th17 response through an innate IFN-γ-IL-27 axis. *J Exp Med* 212(10):1739–1752.
55. Kleiter I, et al. (2007) Inhibition of Smad7, a negative regulator of TGF-beta signaling, suppresses autoimmune encephalomyelitis. *J Neuroimmunol* 187(1-2):61–73.
56. Monteleone G, et al. (2001) Blocking Smad7 restores TGF-beta1 signaling in chronic inflammatory bowel disease. *J Clin Invest* 108(4):601–609.
57. Monteleone G, et al. (2015) Mongersen, an oral SMAD7 antisense oligonucleotide, and Crohn's disease. *N Engl J Med* 372(12):1104–1113.
58. Kim YC, Kim KK, Shevach EM (2010) Simvastatin induces Foxp3+ T regulatory cells by modulation of transforming growth factor-beta signal transduction. *Immunology* 130(4):484–493.
59. Lee HM, et al. (2015) IFNγ signaling endows DCs with the capacity to control type I inflammation during parasitic infection through promoting T-bet+ regulatory T cells. *PLoS Pathog* 11(2):e1004635.
60. Greter M, et al. (2005) Dendritic cells permit immune invasion of the CNS in an animal model of multiple sclerosis. *Nat Med* 11(3):328–334.
61. Prinz M, et al. (2008) Distinct and nonredundant in vivo functions of IFNAR on myeloid cells limit autoimmunity in the central nervous system. *Immunity* 28(5):675–686.